

# Effect of Strong Electron Correlation on the Efficiency of Photosynthetic Light Harvesting

David A. Mazziotti\*

Department of Chemistry and The James Franck Institute, The University of Chicago, Chicago, IL 60637

(Dated: Submitted August 3, 2011; Revised December 6, 2011)

Research into the efficiency of photosynthetic light harvesting has focused on two factors: (1) entanglement of chromophores, and (2) environmental noise. In this Letter efficiency is shown to be equally affected by a third factor: (3) strong electron correlation. While chromophores are conjugated  $\pi$ -bonding molecules with strongly correlated electrons, previous models have not treated this correlation explicitly. Here we generalize the single-electron models to a multi-electron model and show that correlation enhances the energy-transfer efficiency in the model by more than 100%. Implications include insights into the interplay of correlation and entanglement as well as new design principles for energy-efficient materials.

PACS numbers: 31.10.+z

Nature harvests solar energy with a remarkably high *quantum efficiency*, the percentage of charge carriers created by photons. Recent spectroscopic experiments [1–3] and theoretical models [4–13], provide strong evidence that efficient light harvesting in nature occurs by a quantum mechanism involving sustained electronic coherence [14] and entanglement [15, 16] between chromophores. While the chromophores are chlorophyll molecules containing large networks of conjugated carbon bonds that surround a charged magnesium ion, they have largely been represented in theoretical studies [4–13] by one-electron models that neglect the effects of electron correlation and entanglement within chromophores. Two advanced methods in electronic structure, density-matrix renormalization group [17] and two-electron reduced-density-matrix theory [18, 19], have recently shown that networks of conjugated bonds as in acene chains [17, 20], acene sheets [20], and chlorophyll are associated with polyradical character that cannot be adequately described without a strongly correlated many-electron quantum model.

In this Letter we examine the efficiency of light harvesting where we represent each chromophore by a correlated  $N$ -electron model to treat strong electron correlation. Figure 1 illustrates the replacement of one-electron models for each of the 7 chromophores in the Fenna-Matthews-Olson (FMO) complex of green-sulfur bacteria by  $N$ -electron models of increasing complexity. Here we employ the  $N$ -electron Lipkin-Meshkov-Glick (LMG) model [21] used extensively in electronic structure [22–29] and quantum information [16]. We find that strong electron correlation dramatically enhances the efficiency of the energy transfer to the reaction center by more than 100%. Strong electron correlation, the results show, is likely employed by nature to enhance its energy-transfer efficiency as much as other factors such as (i) environmental noise [5–10] and (ii) entanglement between chromophores [11–13], which have been extensively studied in the recent literature. The correlation of electrons within

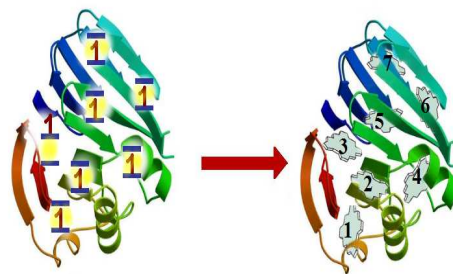


**FIG. 1. Single electrons or correlated chromophores.** Each of the seven chromophores in the FMO complex is generally treated as a single electron in a two-state model (left), and yet the chromophores are constructed from chlorophyll molecules with many strongly correlated electrons (right). Here we treat each of the chromophores by a correlated  $N$ -electron model by Lipkin, Meshkov, and Glick. Illustration by K. Naftchi-Ardebili, The University of Chicago, 2011. Used with permission.

a molecular subunit like a chromophore cannot be separated from their entanglement between molecular subunits. Furthermore, the results suggest a general design principle for man-made materials in which electron correlations and entanglements both within and between subunits are simultaneously tuned for achieving enhanced quantum efficiencies. In combination with other recent advances, including the study of functional subsystems of the FMO complex [4], this interplay of electron entanglements on different length scales may enable us to develop materials with quantum efficiencies approaching those found in natural processes from photosynthesis to bioluminescence.

The Fenna-Matthews-Olson (FMO) complex of green-sulfur bacteria contains three identical subunits, each with a network of seven chromophores. Theoretical models of an FMO complex's subunit typically represent each of the seven chromophore by a *one-electron model* in which the electron has access to two energy levels sep-

arated by the excitation energy of the chromophore. Interactions  $\hat{U}$  between pairs of chromophores are modeled by the exchange of single-electron excitations (or *excitons*) between them:

$$\hat{H} = \hat{H}_0 + \hat{U} \quad (1)$$

where

$$\hat{H}_0 = \frac{1}{2} \sum_{s,m} m \epsilon_s a_{s,m}^\dagger a_{s,m} \quad (2)$$

$$\hat{U} = \sum_{s \neq t} U_{s,t} a_{s,+1}^\dagger a_{s,-1} a_{t,-1}^\dagger a_{t,+1}. \quad (3)$$

The quantum numbers  $s$  and  $t$  denote the seven sites of the chromophores while the quantum number  $m$ , equal to  $+1$  or  $-1$ , indicates one of the two energy levels within each chromophore. The second-quantized operator  $a_{s,m}^\dagger$  ( $a_{s,m}$ ) creates (annihilates) an electron on chromophore  $s$  in energy level  $m$ . The 7 parameters  $\epsilon_s$  are the excitation energies of the chromophore, and the 21 parameters  $U_{s,t}$  are the coupling energies between all pairs of chromophores. Typical values for the excitation and coupling energies are given in the 7x7 Hamiltonian of Ref. [30].

Here we generalize this representation by using the  $N$ -electron LMG model [21]. Each chromophore is modeled as  $N$  electrons in two energy levels that are each  $N$ -fold degenerate; a pairwise interaction scatters two electrons from the lower level to the upper level or from the upper level to the lower level [24]. The Hamiltonian of the 7 interacting LMG chromophores can be expressed as follows:

$$\hat{H} = \hat{H}_0 + \lambda \hat{U} + \hat{V} \quad (4)$$

where

$$\hat{H}_0 = \frac{1}{2} \sum_{s,m,p} m \epsilon_s a_{s,m,p}^\dagger a_{s,m,p}, \quad (5)$$

$$\hat{U} = \frac{1}{N} \sum_{s \neq t,p} U_{s,t} a_{s,+1,p}^\dagger a_{s,-1,p} a_{t,-1,p}^\dagger a_{t,+1,p}, \quad (6)$$

$$\hat{V} = \frac{1}{2} \sum_{s,m,p,q} V a_{s,m,p}^\dagger a_{s,m,q}^\dagger a_{s,-m,q} a_{s,-m,p}, \quad (7)$$

where  $\hat{V}$  accounts for the interactions *within* each chromophore and  $\lambda \in [0, 1]$  is a screening parameter to be defined below. The new quantum number  $p$  (pr  $q$ ) denotes the  $N$  degenerate states within each energy level, which are necessary to accommodate the  $N$  electrons. When the interaction strength  $V$  equals zero, the  $N$  electrons on each site are non-interacting, and the model behaves the same as the one-electron-per-site models; when  $V$  is unequal to zero, we have a generalized model for light harvesting with a tunable electron correlation on the chromophores.

Environmental effects of dephasing and dissipation as well as the transfer of energy to the reaction center (sink)

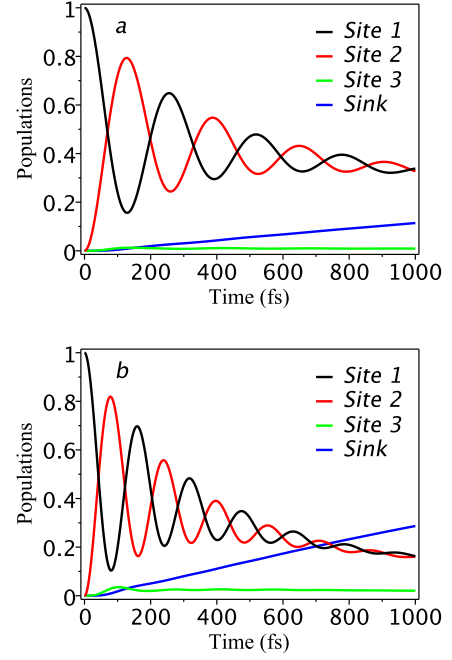


FIG. 2. **Populations of chromophores 1-3 and sink with (b) and without (a) electron correlation per site.** The exciton populations in chromophores 1, 2, and 3 as well as the sink population are shown as functions of time in femtoseconds (fs) for  $N = 4$  with (a)  $V = 0.0$  and (b)  $V = 0.8$ . Correlating the four electrons on each chromophore significantly accelerates the increase in the sink population with time.

can be incorporated by introducing a Lindblad operator  $\hat{L}$  into the *quantum Liouville equation*

$$\frac{d}{dt} D = -\frac{i}{\hbar} [\hat{H}, D] + \hat{L}(D) \quad (8)$$

where  $D$  is the many-electron density matrix. The Lindblad operator can be divided into three operators that account for dephasing, dissipation, and the sink

$$\hat{L}(D) = \hat{L}_{\text{deph}}(D) + \hat{L}_{\text{diss}}(D) + \hat{L}_{\text{sink}}(D) \quad (9)$$

where

$$\hat{L}_{\text{deph}}(D) = \alpha \sum_k 2 \langle k|D|k \rangle |k\rangle \langle k| - \{ |k\rangle \langle k|, D \}, \quad (10)$$

$$\hat{L}_{\text{diss}}(D) = \beta \sum_k 2 \langle k|D|k \rangle |g\rangle \langle g| - \{ |k\rangle \langle k|, D \}, \quad (11)$$

$$\hat{L}_{\text{sink}}(D) = 2\gamma \langle 3|D|3 \rangle |s\rangle \langle s| - \gamma \{ |3\rangle \langle 3|, D \}. \quad (12)$$

The state  $|g\rangle$  denotes the ground eigenstate of the Hamiltonian in Eq. (4), the states  $|k\rangle$  represent the excited eigenstates computed from this Hamiltonian where the interaction  $\hat{U}$  between chromophores is set to zero, the state  $|s\rangle$  denotes the reaction center (sink), and  $|3\rangle$  indicates the first excited state of the third chromophore multiplied by the ground states of the other chromophores.

Non-Markovian effects from the environment can also be added to the quantum Liouville equation (for example, refer to Ref. [10]); however, they will not qualitatively change the effect of strong electron correlation within chromophores on energy-transfer efficiency.

The values for the site excitation energies are defined by the 7x7 Hamiltonian of Ref. [30]; when  $V > 0$ , the parameters  $\{\epsilon_s\}$  are adjusted to ensure that the excitations of the correlated LMG models agree with the excitation energies of the seven chromophores. Selection of the coupling energies  $U_{s,t}$  in Eq. 4) also requires adjustment. Because the coupling energies given in Ref. [30] are “dressed” dipole-dipole interactions that account implicitly for both the electron correlation within the chromophores and the protein environment surrounding the chromophores, they require adjustment for the LMG chromophore model that contains an explicit electron-electron interaction. Previous 2-RDM-based calculations of acene chains and sheets reveal the presence of strong electron correlation in conjugated systems of sizes similar to the bacteriochlorophyll molecules in the FMO complex. Based on acene-chain data [20], we estimate the interaction strength  $V$  with  $N = 4$  to be 0.8, which gives an 80% probability of finding an electron in the highest occupied orbital (occupied in a mean-field treatment) and a 20% probability of finding an electron in the lowest unoccupied orbital. This estimate is conservative because: (i) the acene chains of a similar length typically reveal a nearly biradical filling ( $\approx 50\%$  in the highest occupied orbital), and (ii) the presence of the Mg ion with its  $d$  orbitals is expected to enhance the degree of correlation. To prevent overcounting of the electron correlation’s effect on the coupling, we screen the coupling energies  $U_{s,t}$  of Ref. [30] by selecting  $\lambda$  in Eq. 4) to be less than unity. Specifically, we set  $\lambda = 0.629$  to match experimental data with the LMG model when  $N = 4$  and  $V = 0.8$ . The rate parameters  $\alpha$ ,  $\beta$ , and  $\gamma$  in the Lindblad operators in Eq. 9 are chosen in atomic units to be  $1.52 \times 10^{-4}$ ,  $7.26 \times 10^{-5}$ , and  $1.21 \times 10^{-8}$ , respectively. These definitions are similar to those employed in previous work when  $V = 0$  [30].

The exciton populations in chromophores 1, 2, and 3 as well as the sink population are shown as functions of time in femtoseconds (fs) in Figs. 2a and 2b for  $N = 4$  and  $\lambda = 0.629$  with  $V = 0.0$  and  $V = 0.8$ , respectively. Population dynamics of the excitation are generated by evolving the Liouville equation in Eq. (8) from an initial density matrix with chromophore 1 in its first excited state and the other chromophores in their ground states. Correlating the 4 electrons on each chromophore significantly accelerates the increase in the sink population with time. By 1 ps the sink population for  $V = 0.0$  is 0.114 while the population for  $V = 0.8$  is 0.287. Correlating the excitons on each chromophore also has the effect of shortening the periods of oscillation in chromophores 1 and 2 and accelerating the population decay in these chromophores, which is consistent with the change in the

sink population.

The sink population as a function of time (fs) is shown in Figs. 3 for a range of  $V$  with  $N = 4$  and  $\lambda = 0.629$ . Importantly, as  $V$  increases, we observe a dramatic acceleration of the increase of the sink population. For  $V$  increasing by the sequence 0.0, 0.4, 0.8, and 1.2, the sink population at 2 ps increases by the sequence 0.221, 0.367, 0.498, and 0.547. For  $N = 4$  correlating the electrons within the chromophores significantly increases the efficiency of energy transfer to the reaction center (sink) by as much as 148%. While we choose  $N = 4$ , the number  $N$  of electrons per chromophore can model electron correlation for any  $N > 2$ . The precise value of  $N > 2$  is unimportant because the effect of changing  $N$  can be related to a rescaling of the interaction  $V$ .

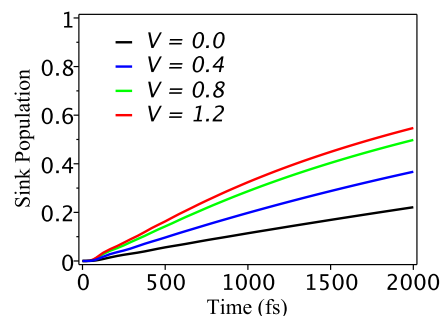


FIG. 3. **Correlation-enhanced transfer to the reaction center.** The reaction center (sink) population as a function of time (fs) is shown in for a range of  $V$  with  $N = 4$ . Correlating the electrons within the chromophores significantly increases the efficiency of energy transfer to the reaction center (sink).

Figure 4 examines the entanglement of excitons between the LMG-model chromophores for  $N = 4$  and  $\lambda = 0.629$  with  $V = 0.0$  and  $V = 0.8$ . We employ a measure of global entanglement in which the squared Euclidean distance between the quantum density matrix and its nearest classical density matrix is computed [26, 31–33]:

$$\sigma(D) = \|D - C\|^2 = \sum_{i,j} |D_j^i - C_j^i|^2. \quad (13)$$

In some cases like the entanglement of the chromophores, the squared Euclidean distance can be viewed as the sum of the squares of the *concurrences* [15], a measure of local entanglement. Within the mathematical framework of Bergmann distances, the squared Euclidean distance can also be related to *quantum relative entropy* [13, 16], which is often applied as a global entanglement measure. The squared Euclidean distance  $\sigma(D)$  is nonzero if and only if the excitons on different chromophores are entangled. The correlation of electrons increases the degree of the entanglement between chromophores at early times and the frequency of its oscillation. The greater entanglement

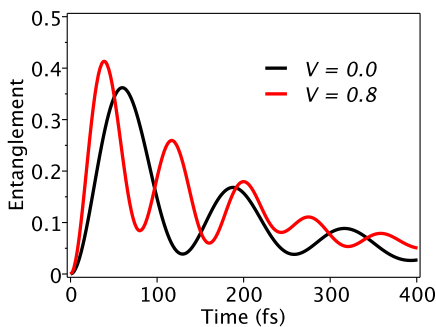


FIG. 4. **Entanglement of excitons with and without electron correlation.** A measure of global entanglement is shown as a function of time (fs) for  $N = 4$  with  $V = 0.0$  and  $V = 0.8$ . The correlation of the excitons increases the degree of the entanglement between chromophores at early times and the frequency of its oscillation.

at early times reflects the opening of additional channels between chromophores for quantum energy transfer.

The chromophores interact through intermolecular forces, both dipole-dipole and London dispersion forces. The present results imply that nature enhances these intermolecular forces through strong electron correlation in the  $\pi$ -bonded networks of the chromophores to achieve the observed energy-transfer efficiency. The two parameters of the LMG chromophore model provide the simplest approach to studying the effect of strong electron correlation  $V$  on the effective coupling between chromophores. The one-electron or dipole models with their coupling energies  $U_{s,t}$  can mimic the efficiency from such correlation within chromophores through an empirical inflation of the one-electron  $U$  coupling, but they do not provide a mechanism for either isolating or estimating the magnitude of the enhanced coupling due to strong electron correlation. Orbital occupations from recent 2-RDM calculations of correlation in polyaromatic hydrocarbons [20] suggest  $V = 0.8$  to be a conservative estimate of the correlation within the LMG models of the 7 chromophores. Using this estimate with coupling energies screened to match experimental and computational data, we observe a greater than 100% enhancement from the strong electron correlation.

Correlation-enhanced energy transfer can be compared with noise-assisted transfer. Theoretical models [5–9, 12, 13] have shown that noise from the environment (dephasing) can assist energy transfer in the FMO complex by interfering with the coherence (resonance) between chromophores with similar energies, which facilitates the downhill flow of energy to the lowest-energy, third chromophore, connected to the reaction center. Electron correlation on each chromophore, we have shown, enhances transfer by opening additional coherent channels between chromophores, which also accelerates en-

ergy transfer to the third chromophore. Photosynthesis can draw from both of these sources, strong electron correlation within chromophores and environmental noise, to increase the rates of energy transfer. Some of the experimental energy-transfer efficiency attributed to noise in one-electron chromophores models may in fact be due to strong electron correlation.

Briggs and Eisfeld [12] recently examined whether the energy-transfer efficiency from quantum entanglement might be matched by a purely classical process. They conclude that if chromophores are approximated as dipoles, then quantum and classical treatments can achieve similar efficiency. While their result might also be extendable to other dipole or one-electron approximations of the chromophores, many-electron models of the chromophores cannot be represented within classical physics. Neither the electron correlation, present in the LMG model of the chromophores when  $V > 0$ , nor the associated enhancement of energy-transfer efficiency can be mapped onto an analogous classical process.

Many theoretical models [5–9, 12, 13] have been designed to explore the energy transfer in recent light-harvesting experiments, but most of them treat each chromophore by a single electron with two possible energy states. In reality, however, the chromophores are assembled from chlorophyll molecules that contain an extensive network of conjugated carbon-carbon bonds surrounding magnesium ions, from which significant strong electron correlation, including polyradical character, has been shown to emerge [17, 20]. In this Letter we have examined the effect of strong electron correlation and entanglement *within* chromophores through an extension of single-electron models of the chromophores to  $N$ -electron models, based on the LMG model [16, 21, 24, 26]. We find that increasing the degree of electron correlation of each LMG-model chromophore significantly enhances the efficiency with which energy is transferred to the reaction center (sink). This result, showing that nature likely uses strong electron correlation to achieve its energy-transfer efficiency, also has implications for the design of more energy- and information-efficient materials.

DAM gratefully acknowledges the ARO Grant No. W91 INF-1 1-1-0085, NSF CAREER Grant No. 0644888, Microsoft Corporation, Dreyfus Foundation, and David-Lucile Packard Foundation for support.

---

\* damazz@uchicago.edu

- [1] G. S. Engel, T. R. Calhoun, E. L. Read, T. K. Ahn, T. Mancal, Y. C. Cheng, R. E. Blankenship, and G. R. Fleming, *Nature* **446**, 782 (2007).
- [2] E. Collini, C. Y. Wong, K. E. Wilk, P. M. G. Curmi, P. Brumer, and G. D. Scholes, *Nature* **463**, 644 (2010).
- [3] G. Panitchayangkoon, D. Hayes, K. A. Fransted, J. R. Caram, E. Harel, J. Z. Wen, R. E. Blankenship, and G. S.

- Engel, Proc. Natl Acad. Sci. USA **107**, 12766 (2010).
- [4] N. Skochdopole and D. A. Mazziotti, J. Phys. Chem. Lett. **2**, 2989 (2011).
  - [5] J. S. Cao and R. J. Silbey, J. Phys. Chem. A **113**, 13825 (2009).
  - [6] F. Caruso, A. W. Chin, A. Datta, S. F. Huelga, and M. B. Plenio, Phys. Rev. A **81**, 062346 (2010).
  - [7] P. Huo and D. F. Coker, J. Chem. Phys. **133**, 184108 (2010).
  - [8] D. P. S. McCutcheon and A. Nazir, Phys. Rev. B **83**, 165101 (2011).
  - [9] B. Palmieri, D. Abramavicius, and S. Mukamel, J. Chem. Phys. **130**, 204512 (2009).
  - [10] J. Zhu, S. Kais, P. Rebentrost, and A. Aspuru-Guzik, J. Phys. Chem. B **115**, 1531 (2011).
  - [11] K. Bradler, M. M. Wilde, S. Vinjanampathy, and D. B. Uskov, Phys. Rev. A **82**, 062310 (2010).
  - [12] J. S. Briggs and A. Eisfeld, Phys. Rev. E **83**, 051911 (2011).
  - [13] M. Sarovar, A. Ishizaki, G. R. Fleming, and K. B. Whaley, Nature Physics **6**, 462 (2010).
  - [14] C. Brif, R. Chakrabarti, and H. Rabitz, New J. Phys. **12**, 075008 (2010).
  - [15] S. Kais, Adv. Chem. Phys. **134**, 493 (2007).
  - [16] R. Horodecki, P. Horodecki, M. Horodecki, and K. Horodecki, Rev. Mod. Phys. **81**, 865 (2009).
  - [17] J. Hachmann, J. J. Dorando, M. Avilés, and G. K. Chan, J. Chem. Phys. **127** (2007).
  - [18] D. A. Mazziotti, Phys. Rev. Lett. **106**, 083001 (2011).
  - [19] R. M. Erdahl, Adv. Chem. Phys. **134**, 61 (2007).
  - [20] G. Gidofalvi and D. A. Mazziotti, J. Chem. Phys. **129**, 134108 (2008); K. Pelzer, L. Greenman, G. Gidofalvi, and D. A. Mazziotti, J. Phys. Chem. A **115**, 5632 (2011).
  - [21] H. J. Lipkin, N. Meshkov, and A. J. Glick, Nucl. Phys. **62**, 188 (1965).
  - [22] J. Arponen and J. Rantakivi, Nucl. Phys. A **407**, 141 (1983).
  - [23] R. Perez, M. C. Cambiaggio, and J. P. Vary, Phys. Rev. C **37**, 2194 (1988).
  - [24] D. A. Mazziotti, Phys. Rev. A **57**, 4219 (1998); Chem. Phys. Lett. **289**, 419 (1998).
  - [25] J. Stein, J. Phys. G **26**, 377 (2000).
  - [26] D. A. Mazziotti and D. R. Herschbach, Phys. Rev. A **62**, 043603 (2000).
  - [27] K. Yasuda, Phys. Rev. A **65**, 052121 (2002).
  - [28] D. A. Mazziotti, Phys. Rev. A **69**, 012507 (2004).
  - [29] G. Gidofalvi and D. A. Mazziotti, Phys. Rev. A **74**, 012501 (2006).
  - [30] A. W. Chin, A. Datta, F. Caruso, S. F. Huelga, and M. B. Plenio, New J. Phys. **12**, 065002 (2010).
  - [31] A. O. Pittenger and M. H. Rubin, Lin. Alg. Appl. **346**, 47 (2002).
  - [32] R. A. Bertlmann, H. Narnhofer, and W. Thirring, Phys. Rev. A **66**, 032319 (2002).
  - [33] J. E. Harriman, Phys. Rev. A **17**, 1249 (1978).